Journal of Pharmaceutical and Biomedical Analysis 56 (2011) 183–190

Contents lists available at ScienceDirect

Journal of Pharmaceutical and Biomedical Analysis

journal homepage: www.elsevier.com/locate/jpba

Analysis of co-spray-dried meloxicam–mannitol systems containing crystalline microcomposites

Anita Pomázi, Rita Ambrus, Péter Sipos, Piroska Szabó-Révész*

Department of Pharmaceutical Technology, University of Szeged, Eötvös 6, H-6720 Szeged, Hungary

ARTICLE INFO

Article history:
Received 11 March 2011
Received in revised form 9 May 2011
Accepted 10 May 2011
Available online 17 May 2011

Keywords:
Dissolution rate
Microparticles
Spray-drying
Poorly soluble drug
Powder technology
Morphology

ABSTRACT

The crystal size, form, wettability and rate of dissolution of a drug are factors limiting its nasal or pulmonary administration. The aim of this work was to achieve an ideal crystal habit, good wettability and the rapid release of meloxicam (MEL), a poorly water-soluble non-steroidal anti-inflammatory drug. The structures of MEL and the carrier-based systems were analysed by differential scanning calorimetry, X-ray diffractometry and Fourier transform infrared spectroscopy. The particle size and morphology were investigated by laser diffraction and SEM analyses. The novelty of this work was the use of a co-spray-drying technique, which resulted in mannitol-based crystalline microcomposites (1–6 μm) containing MEL microcrystals (1–5 μm). The particle size and form of the MEL microcrystals were adjusted by a top-down method. The presence of mannitol (with a MEL:mannitol mass ratio of 1:1) with additives ensured the homogeneous distribution of MEL in the microcomposites with good wettability and rapid release (100% MEL within 5 min).

1. Introduction

The bioavailability of poorly water-soluble or insoluble drugs is a well-known difficulty in the development of many pharmaceutical products. In general, the solubility properties and the rate of dissolution of active pharmaceutical ingredients (APIs) impact the bioavailability of the product [1,2]. Incomplete wettability, sparing water-solubility, a low dissolution rate and poor permeability can result in low bioavailability and an inadequate therapeutic effect [3].

Non-steroidal anti-inflammatory drugs (NSAIDs) are currently the most widely prescribed medication. During the formulation of NSAIDs, it is strategically important to solve their solubility problems, which can lead to decreases in the drug quantity, applied and unwanted side-effects, together with an improvement of their bioavailability [4,5]. A number of advanced technological methods are available with which to modify the physico-chemical properties and increase the rate of dissolution of NSAIDs. The most common technologies are particle size reduction [6,7], co-crystallization [8], cyclodextrin inclusion complexation [9,10], the use of inert water-soluble drug carriers in solid solutions or dispersions [11], the production of a suspension by a solvent evaporation method [12] and the preparation of nanocrystalline or amorphous forms of APIs [13]. Many pharmaceutical and biochemical products are spray-dried, a process currently receiving great attention as concerns the drying of preformed microcrystals. When a suspension of drug crystals in a polymer solution is spray-dried, microcapsulated particles are prepared, whereas the spray-drying of a polymer solution containing dissolved drug leads to the formation of drug-containing microspheres in which the drug can be dispersed as microcrystals [14–17].

Meloxicam (MEL) is practically insoluble in water. It can be graded in Class II of the Biopharmaceutical Classification System, which means low aqueous solubility and rapid absorption from the intestinal tract (high permeability). MEL has anti-inflammatory and analgetic therapeutic effects. It is frequently used to treat rheumatoid arthritis, osteoarthritis and other joint diseases, e.g., Alzheimer's disease and cancer [18–21]. MEL is a commonly applied NSAID, because it does not cause an aspirin-like hypersensitivity reaction [22]. Increase of the extent of its dissolution is of strategic importance, as the dose-dependent side-effects may thereby be reduced and the therapeutic efficacy increased. The rate of dissolution of MEL can generally be improved by applying formulation techniques, such as the preparation of binary systems with a hydrophilic carrier, by mixing, melting or solvent methods, including particle size modification [23–25]. Naidu et al. utilized cyclodextrins to enhance the dissolution properties of MEL [26]. This formulation possibility can be applied for the oral administration route for solid dosage forms, where a high proportion of carrier is needed to prevent the agglomeration of the micronized active ingredient. Nassab et al. found that the use of melt technology for the regular dissolution of MEL resulted in mixed microcrystals.

* Corresponding author. Tel.: +36 62 545575, fax: +36 62 545571.
E-mail address: revesz@pharm.u-szeged.hu (P. Szabó-Révész).

0731-7085/$ – see front matter © 2011 Elsevier B.V. All rights reserved.
doi:10.1016/j.jpba.2011.05.008

However, this technology was carried out with 10 parts of mannitol (M) and 1 part of MEL [25]. The frequently used particle-size reduction techniques such as ball and jet milling are disadvantageous for this active substance [27]. To achieve uniform particle size and to prevent the aggregation of reduced particles, the application of a carrier-based spray-drying technique containing additives may be necessary. Different carriers (e.g., microcrystalline cellulose, lactose monohydrate, M, sorbitol, cyclodextrin, xylitol, glucose, raffinose and trehalose) are used to ensure the distribution of APIs [28]. M has attracted attention as the most popular substance used in complex systems to increase the rate of dissolution of APIs [29]. It is advantageous as a highly water-soluble compound with low toxicity, low hygroscopicity and significant stability [30].

MEL can be administrated by the nasal route for local analgesic, anti-inflammatory and systemic effects [31]. Pulmonary application is a novelty for local and systemic treatment, used for the mono- and combination treatment of cancer, pulmonary fibrosis, inflammation and pain [32–35]. For both nasal and pulmonary applications, appropriate particle size (1–5 μm) [36,37] and form are required to ensure adequate physico-chemical properties [38,39], the most important condition is rapid drug release, because of the short duration of API retention on the mucosa. A solid dosage form is suitable for these routes, where the main requirements are optimum particle size and form, wettability and rapid dissolution. One disadvantage of micronized APIs is their tendency to aggregate. The application of carriers can ensure appropriate distribution of the substance. However, a high amount of carrier can give rise to problems during application [40]. PVP K-25 and Tween 80 may be safely applied for pulmonary and nasal use as additives (stabilizer and wetting agent); toxic effects are not detected in the respiratory tract [41,42]. In our previous work, we investigated the cytotoxicity of these carrier-based microcomposites on Calu-3 lung epithelial cells to predict the applicability of the products and determine the optimum product concentration in the lung [43].

The crystal habit (i.e., size and shape), wettability and rate of dissolution of MEL are the primary factors limiting its formulation for nasal and pulmonary administration [44,45]. In particle engineering, co-spray-drying is a one-step process which can be used as a formulation platform to improve the particle habit of formulations containing API and excipients together. The main advantage of co-spray-drying is the improvement of the processability and bioavailability of APIs through the production of spherical particles coated by additives [46,47].

The primary aim of our research, therefore, was to achieve an adequate crystal habit, good wettability and the rapid release of MEL. Another objective was to reduce the amount of the water-soluble carrier M required for the homogeneous distribution of the API. The novelty of this work was the use of a carrier-based co-spray-drying technique to produce MEL–M crystalline microcomposites containing MEL microcrystals.

2. Materials and methods

2.1. Materials

Meloxicam (4-hydroxy-2-methyl-N-(5-methyl-2-thiazolyl)-2H-benzothiazine-3-carboxamide-1,1-dioxide) (MEL) was from EGIS Ltd. (Budapest, Hungary). Polyvinylpyrrolidone K-25 (PVP) was from ISP Customer Service GmBH (Köln, Germany), and Tween 80 (polysorbate 80) (T) and β-D-mannitol (M) were from Hungaropharma Rt (Budapest, Hungary).

Table 1
Compositions of samples.

Sample	MEL (g)	M (g)	T (g)	PVP (g)
MEL	1	–	–	–
MEL spd	1	–	–	–
M	–	1	–	–
M spd	–	1	–	–
MEL–M	1	1	–	–
MEL–M–T	1	1	0.1	–
MEL–M–PVP	1	1	–	0.05
MEL–M–T + PVP	1	1	0.1	0.05

2.2. Methods

2.2.1. Preparation of co-spray-dried products containing MEL

A microsuspension was prepared from 1 g each of MEL and M, 0.1 g of T and/or 0.05 g of PVP, made up to 20 g with water, using an Ultraturrax (UT) (T-25, IKA-WERKE, Germany) at 6500 and 24,000 rpm for 10 min, and for spray-drying a Büchi Mini Dryer B-191 (Switzerland) with 130 °C inlet and 70 °C outlet temperature; the aspirator capacity was 60%, the aspirator pressure was −25 mbar, the feed rate was 0.065 l h^{-1} and the flow rate was 700 l h^{-1}. Spray-dried MEL (MEL spd) and M (M spd) were prepared as controls from 1 g of MEL or M, made up to 20 g with water, using the same preparation parameters as for the products (Table 1).

Fig. 1 shows the preparation protocol for the carrier-based co-spray-dried systems. In top-down technology drug particles are subsequently broken down by using disintegration methods until

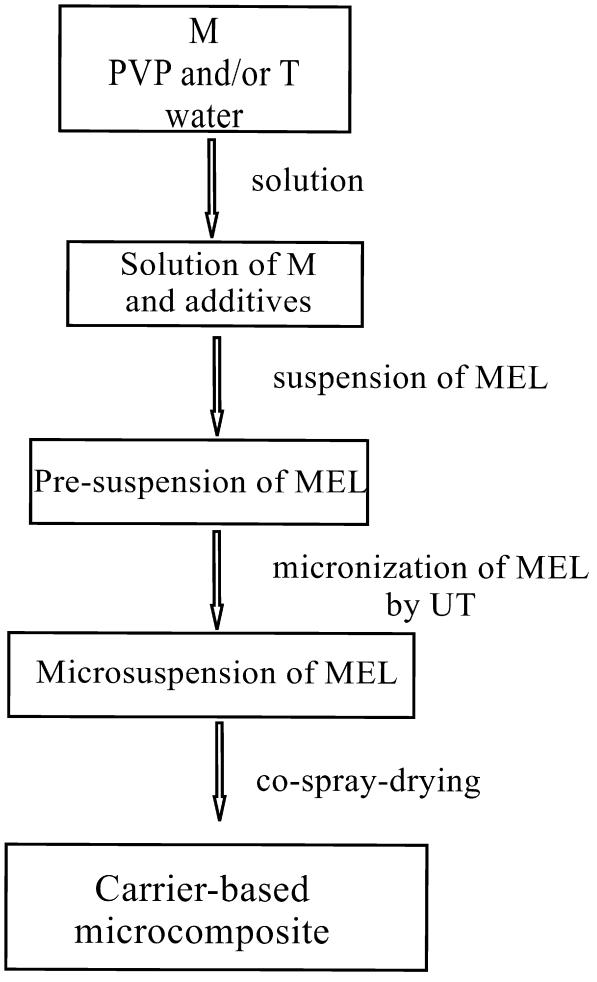

Fig. 1. Preparation protocol for carrier-based microcomposites.

micronized particles are produced. The particle size and shape of the MEL crystals were also modified by applying the top-down method with the Ultraturrax and with the spray-dryer. First, a solution of carrier (M) and additives (T and PVP) was prepared, and then with added MEL, a presuspension was formed. High-shear mixing was carried out at 24,000 rpm. The resulting sample contained the API in suspended form. During co-spray-drying, solid products were obtained, comprising microparticles containing MEL crystals in micronized form.

2.2.2. Preparation of physical mixtures containing MEL

Physical mixtures (PMs) were prepared by Turbula mixer at 50 rpm for 10 min in the same ratios as by sample preparation. The nomenclature followed the system of Table 1. PM was applied as a control by differential scanning calorimetry, hot-stage microscopy and X-ray powder diffraction. To control how the excipients improve the dissolution, the PMs were also investigated.

2.2.3. Particle size analysis

The LEICA Image Processing and Analysis System (LEICA Q500MC, LEICA Cambridge Ltd., England) was used to measure the particle size distribution of spray-dried products including all of the applied components. We compared the products with the pure drug, using 1000 particles per sample.

To compare the size and the size distribution of the individual particles of raw MEL with the MEL in the samples, the products were dispersed in water, using an ultrasonic bath for 2 min. The water soluble components were really dissolved out from the systems and the volume particle-size distribution of MEL was measured by laser diffraction (Mastersizer S, Malvern Instruments Ltd., UK), with the following parameters: 300RF lens; small volume dispersion unit (1000 rpm); true density of MEL 1.565 g cm^{-3} (AccuPyc 1330, Micromeritics, USA); the refractive index for dispersed particles was 1.596 and that for the dispersion medium was 1.330. Laser diffractometry yields the volume size distribution, with particle measurement in the size range 0.1–2000 μm.

2.2.4. Scanning electron microscopy (SEM)

The morphology of the particles was examined by SEM (Hitachi S4700, Hitachi Scientific Ltd., Japan). A sputter coating apparatus (Bio-Rad SC 502, VG Microtech, England) was applied to induce electric conductivity on the surface of the samples. The air pressure was 1.3–13.0 mPa.

2.2.5. Differential scanning calorimetry (DSC)

The DSC measurements were made with a Mettler Toledo DSC 821^e thermal analysis system with the STAR^e thermal analysis program V9.1 (Mettler Inc., Schwerzenbach, Switzerland). Approximately 2–5 mg of MEL or its product was examined in the temperature range between 25 °C and 300 °C. The heating rate was 5 °C min^{-1}. Argon was used as carrier gas, at a flow rate of 10 l h^{-1} during the DSC investigation. A physical mixture in 1:1 mass ratio (PM–MEL–M) was applied as a control sample. The individual components were mixed in a Turbula mixer (Turbula WAB, Systems Schatz, Switzerland) at 50 rpm for 10 min.

2.2.6. Hot-stage microscopy (HSM)

HSM observations of the morphological features and their changes during heating were carried out with a Leica Thermomicroscope (Leica MZ 6, Germany). The samples were observed under the microscope at a scanning speed of 2 °C min^{-1}. The magnification in the photographs was 59.7×.

2.2.7. X-ray powder diffraction (XRPD)

The physical states of the MEL and M in the different samples were evaluated by XRPD with a Miniflex II X-ray Diffractometer (Rigaku Co., Tokyo, Japan), where the tube anode was Cu with Kα = 1.5405 Å. Patterns were collected with a tube voltage of 30 kV and a tube current of 15 mA in step scan mode (4° min^{-1}). The instrument was calibrated by using Si. A physical mixture in 1:1 mass ratio (PM–MEL–M) was applied as a control sample, prepared as before.

2.2.8. Fourier transform infrared spectroscopy (FT-IR)

FT-IR spectra were measured on an Avatar 330 FT-IR apparatus (Thermo Nicolet, USA), in the interval 400–4000 cm^{-1}, at an optical resolution of 4 cm^{-1}. Standard KBr pellets were prepared from 150 mg of KBr pressed at 10 t and samples containing 0.5 mg of MEL.

2.2.9. Wettability: contact angle and polarity

The OCA Contact Angle System (Dataphysics OCA 20, Dataphysics Inc., GmbH, Germany) was used for studies of the wettability of the carrier systems, and products containing MEL. 0.15 g of powder was compressed under a pressure of 1 t by a Specac hydraulic press (Specac Inc., USA). The wetting angles of the pressings were determined after 4.3 μl of distilled water had been dropped onto the surface of the pressings. The change in the wetting angle was registered from 1 to 25 s (minimum of 5 parallel numbers), using the circle fitting method of the OCA System. The method of Wu was applied, in which two liquids with known polar (γ_l^p) and dispersion (γ_l^d) components are used for measurement. The solid surface free energy is the sum of the polar (γ^p) and nonpolar (γ^d) components, and is calculated according to the following equation:

$$(1 + \cos\ \Theta)\gamma_l = \frac{4(\gamma_s^d \gamma_l^d)}{\gamma_s^d \gamma_l^d} + \frac{4(\gamma_s^p \gamma_l^p)}{\gamma_s^p \gamma_l^p}$$

where Θ is the contact angle, γ_s is the solid surface free energy and γ_l is the liquid surface tension. The percentage polarity can be calculated from the γ^p and γ values: $(\gamma^p/\gamma) \times 100$. The liquids used for our contact angle measurements were bidistilled water (γ^p = 50.2 mN m^{-1}, γ^d = 22.6 mN m^{-1}) and diidomethane (γ^p = 1.8 mN m^{-1}, γ^d = 49 mN m^{-1}) [48,49].

2.2.10. Drug content and in vitro dissolution test

The MEL contents in the dried samples were determined by dissolving 100 mg of dried sample in 100 ml of phosphate buffer solution (pH 7.4 ± 0.1), stirring the solution with a magnetic stirrer (400 rpm) at room temperature for 24 h, filtering and analysing spectrophotometrically at 362 nm. Each sample was prepared and analysed in triplicate. The modified paddle method (100 ml media was used instead of 900 ml, therefore the size of paddles and glass container was decreased) of with the USP dissolution apparatus (USP rotating-basket dissolution apparatus, type Pharma Test, Heinburg, Germany) was used to examine MEL and the products. The medium was phosphate buffer with pH 7.4 ± 0.1. The paddle was rotated at 100 rpm and sampling was performed up to 120 min. After filtration (the pore size in filtration was 0.45 μm applying a Millex-HV syringe driven filter unit, Millipore Corporation, Bedford, USA) and dilution, the MEL contents of the samples were determined by spectrophotometry at 362 nm.

3. Results and discussion

3.1. Particle size and morphology (SEM)

The *particle size analysis* revealed that the crystal sizes of the MEL crystals and its products were decreased significantly (Table 2). The size of the raw MEL crystals was 85 μm, i.e., nearly the same as for M. The particle size of the MEL was first decreased with the Ultraturrax in an aqueous suspension without additives. After spray-drying

Table 2
Particle sizes of samples and MEL in products.

Sample	Particle size of samples [μm]	SD [±]	Particle size of MEL in samples [μm]	SD [±]
MEL	85.4	6.6	–	–
MEL spd	19.1	2.6	–	–
M	86.7	5.1	–	–
M spd	1.6	0.8	–	–
MEL–M	1.4	0.3	4.1	3.5
MEL–M–T	4.1	2.0	1.8	0.3
MEL–M–PVP	4.1	1.8	2.9	0.5
MEL–M–T + PVP	5.2	4.0	3.0	0.3

of the aqueous suspension of the MEL, the size was decreased only to 19 μm (MEL spd), because of the poor wettability and aggregation of MEL. Spray-drying of the aqueous solution of M resulted in a size of 1.6 μm (M spd). In the presence of M and additives (wetting and protecting agents), the decrease in the particle size of MEL (UT) was controlled to yield the 1–5 μm range in the microsuspension. After spray-drying, the average particle size of the composites (MEL–M-additives) did not exceed the acceptable range (1–7 μm), and additionally the MEL particle size was optimized (1–5 μm) as in the microsuspension. It is interesting to compare the size of MEL–M (1.4 μm) with that of extracted MEL (4.1 μm), which reflected the aggregation of MEL. Overall, the MEL crystal size was decreased during the process to 5 μm, and the co-spray-drying (the recrystallization of M and the presence of T and PVP) led to optimization of the particle size of the composites (samples) in several pharmaceutical formulations. During our preliminary experiments ratios of MEL:M between 1:0.5 and 1:10 were investigated. The 1:1 mass ratio of MEL and M was ideal.

The *SEM pictures* demonstrate the changes in habit of the crystals (Fig. 2). The large, anisodimensional pure MEL crystals (A) have a smooth surface with a regular prismatic form, whereas the M crystals have an irregular shape with a rough surface (B). Spray-drying led to significantly smaller particles in both cases. Since the size of the MEL crystals in the suspension was decreased by the Ultraturrax, the dried MEL crystals (MEL spd) had the same shape as the raw particles; only the size was changed (C). On the other hand, when M was dissolved in water and recrystallized, the product displayed a changed habit as concerns form and size (M spd) (D).

Fig. 3 shows the habit of the co-spray-dried products. The particles with optimized size were nearly regular and spherical or covered by PVP which resulted in macromolecular film on the MEL–M surface (C and D). In the case of T, deformed particles were seen among the regular particles (B). Uneven surface with crumpling was observed on the MEL–M–T in consequence of the crystallization inhibitory effect of T. The application of PVP led to the best morphological characters (shape and size) for the products if the nasal or pulmonary application is used [51].

3.2. Structural analysis (DSC, HSM, FT-IR, XRPD)

DSC was employed to investigate the crystallinity and the melting of MEL and M in the pure forms, PM–MEL–M (as a control) and co-spray-dried products. The DSC analysis indicated that the raw materials were crystalline, with sharp melting points (Fig. 4). The DSC curves of the original compounds exhibited a sharp endothermic peak at 166 °C, corresponding to the melting point of M, and a

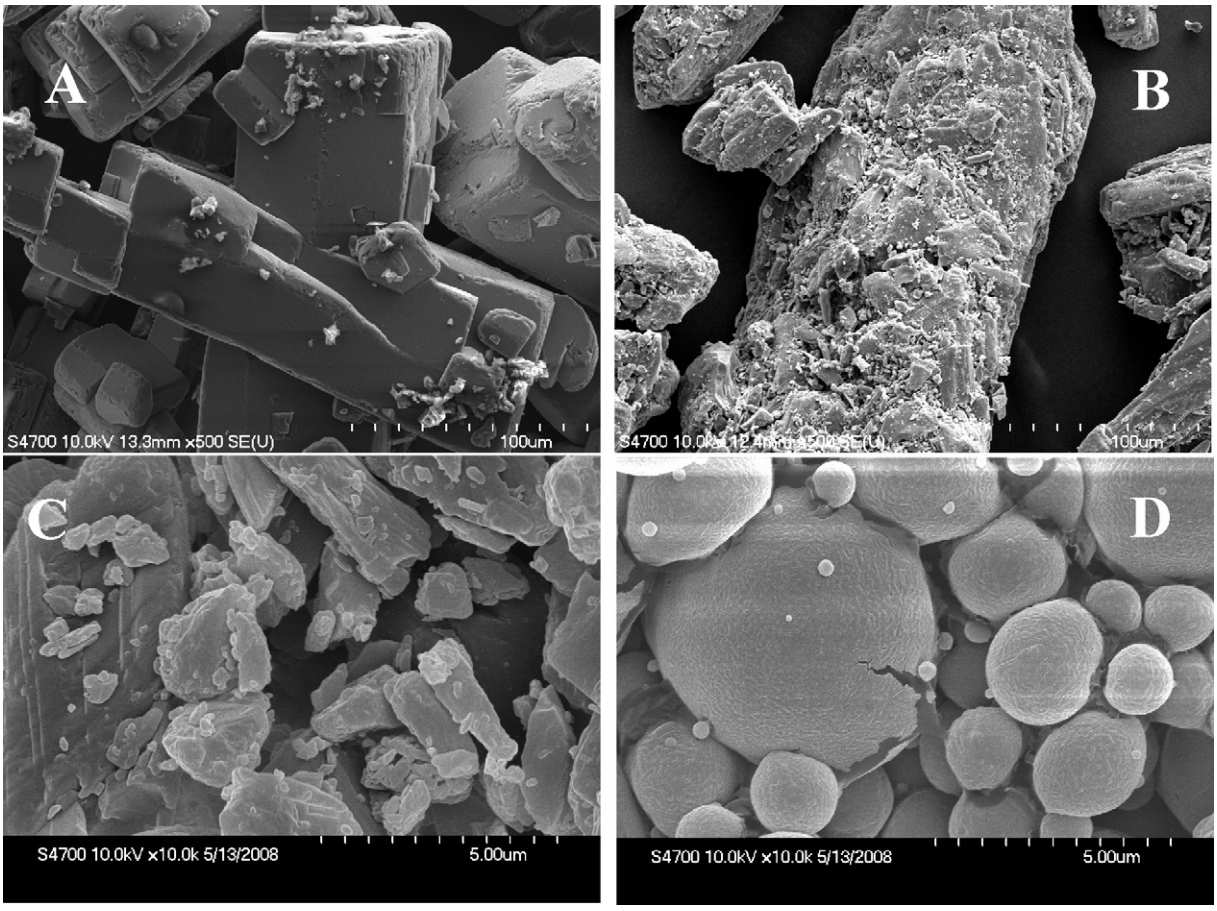

Fig. 2. SEM pictures of MEL (A), M (B), MEL spd (C) and M spd (D).

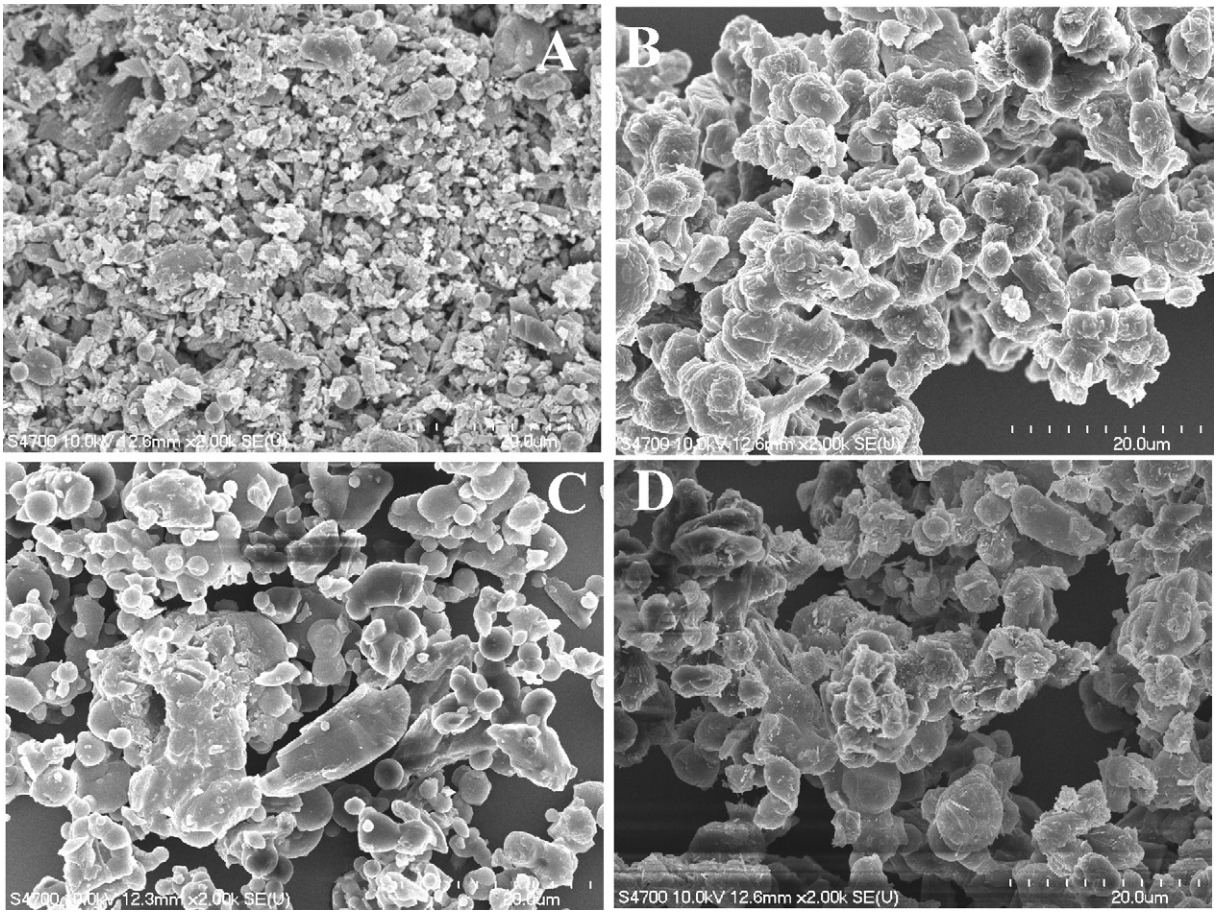

Fig. 3. SEM images of co-spray-dried products MEL–M (A), MEL–M–T (B), MEL–M–PVP (C) and MEL–M–T + PVP (D).

peak at 258 °C, the melting point of MEL. The melting point of MEL was followed by an exothermic peak, which reflects the decomposition of the MEL. The curve of PM–MEL–M indicated significantly lower melting for MEL. As a particle size decrease was not attained by physical mixing, an interaction between MEL and M was presumed on heating in the DSC apparatus. Some of the MEL crystals were dissolved in the melted M because of the heating. For the co-spray-dried products, melting was observed at around 230 °C, i.e., 25 °C lower than the original melting point of the drug (Fig. 5). The enthalpy of MEL in the products was decreased to compare with the raw MEL and MEL in the PM–MEL–M, indicating the dissolution of some of the MEL crystals, similarly as in PM–MEL–M. However, according to the DSC measurements, we could detect the crystalline form of MEL after co-spray-drying. Because of the lower inlet and outlet temperatures (130 °C and 60 °C) on drying, the M could not melt and therefore the MEL crystals could not dissolve in melted M during the procedure.

HSM was applied to visualize the changes in the co-spray-dried products during heating was presented by DSC. This technique is complementary to DSC and may facilitate the interpretation of the DSC results. The thermomicroscopic pictures revealed that the MEL particles were dissolved in the melted M (Fig. 6). With increase of temperature, first the melting of M was detected at 165 °C. At around 170 °C, the MEL crystals started to dissolve/melt at 220–228 °C, before the true melting point (30 °C lower), and com-

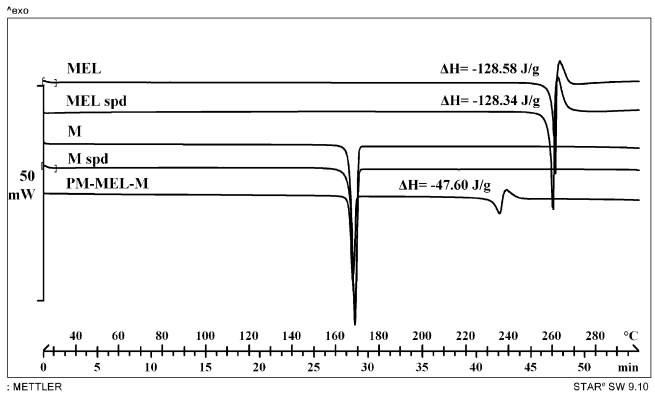

Fig. 4. DSC curves of MEL, MEL spd, M, M spd and PM–MEL–M.

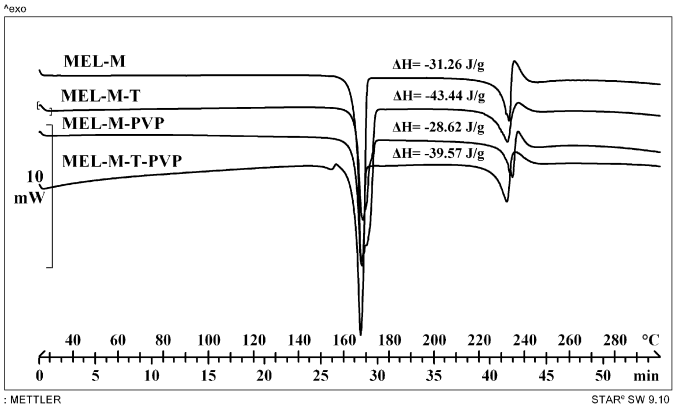

Fig. 5. DSC of co-spray-dried products.

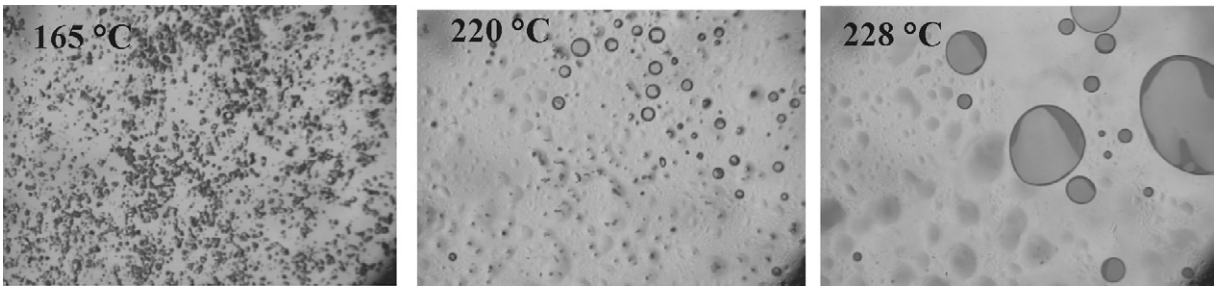

Fig. 6. Thermomicroscopic pictures of MEL with M in a ratio of 1:1.

plete melting was detected, i.e., the DSC curves revealed the earlier melting of MEL.

The presence of numerous distinct peaks in the XRPD spectrum (Fig. 7) indicates that MEL is a crystalline material; its characteristic peaks appear at diffraction angles 2Θ of 13.22, 15.06, 26.46 and 26.67°. After the sample preparation, the crystalline form remained the same for MEL. The characteristic peaks of β-M clearly appeared at diffraction angles 2Θ of 10.62, 14.74, 16.9, 21.15, 23.9 and 29.54°. The M spd contained peaks and patterns for α-M: 9.78, 13.98, 17.44, 20.14, 21.46 and 27.3. The XRPD curve of investigated PM–MEL–M contains characteristic peaks of β-M and MEL. The raw MEL and the co-spray-dried MEL composites displayed similar X-ray diffraction patterns (Fig. 8). This means that the crystalline form of the micronized MEL was not changed by the drying procedure. The polymorphic form of M was detected after the water evaporation. Patterns for α-M were also found in the samples with PVP and/or T.

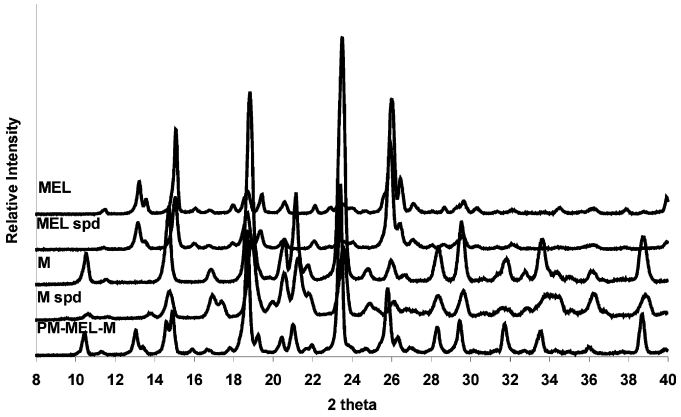

Fig. 7. XRPD patterns of raw materials and PM–MEL–M.

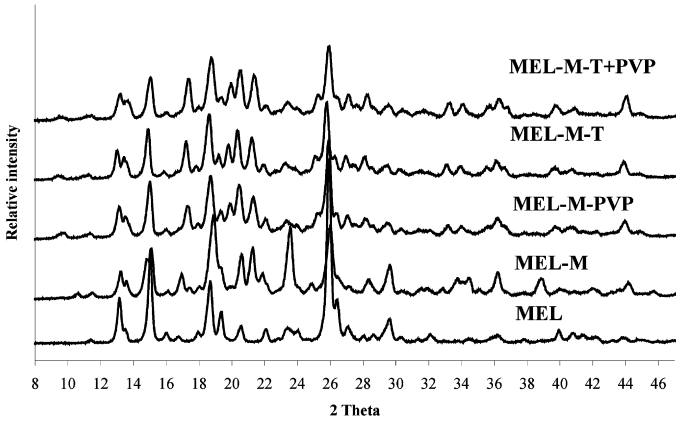

Fig. 8. XRPD patterns of MEL and its products.

The *FT-IR spectrum* of MEL (Fig. 9) exhibited distinct peaks at 3291 cm^{-1}, 1620 cm^{-1} (N–H) and 1580 cm^{-1} (C–O). In the prepared samples, MEL has a crystalline form, i.e., its micronization and co-spray-drying process did not result in an amorphous product. Shifts in the bands were not observed, which means that there was no chemical interaction between the MEL and the additives. For M, several polymorphic forms have been described [25,50]. The FT-IR spectra of the two modifications differ considerably, reflecting the different interaction forces between the various conformational arrangements of the molecules. During the preparation of these co-spray-dried systems, two forms (originally β and after spray-drying α) of M were analysed. The spectral changes were evaluated by subtraction of the PVP and Tween 80 spectra from the spectra of the samples prepared by co-spray drying. Significant differences were seen (Fig. 9) in the FT-IR spectra of the M modifications in the carrier systems, with differences in the C–H deformation vibrations between 1450 and 1200 cm^{-1}. Other significant shifts were detected for the vibrations involving the stretching of the C–O bond (1200–1450 cm^{-1}). The corresponding IR spectra for α-M can be seen in the sample patterns at 952 cm^{-1} and for β at 1419 cm^{-1}, as before.

3.3. Wettability, drug content and in vitro dissolution tests

The *wettability study* (Table 3) indicated that the products (microcomposites) had a more hydrophilic character as compared with MEL. Significantly lower contact angles with water were measured for all samples, the decrease ranging from 52° to 22°. The contact angle of MEL (75°) was relatively high, showing its poor hydrophilicity. Following spray-drying, the MEL particle size was decreased significantly, from 85 to 19 μm (Table 2), but the wettability did not change significantly (72°). As concerns the co-spray-dried products, MEL had a contact angle of 54.9° because of the wetting character of M. With T, we observed nearly the same

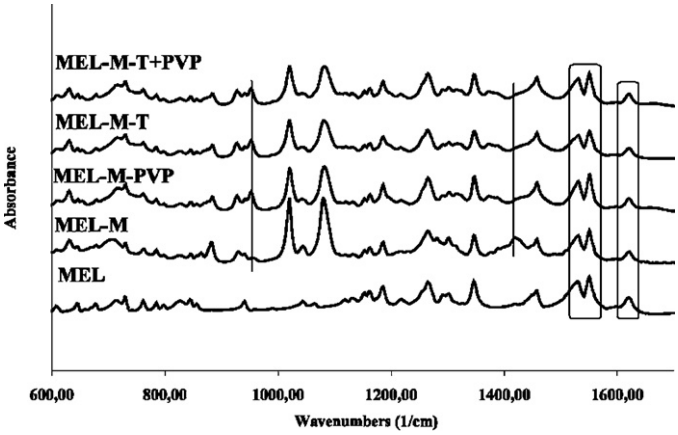

Fig. 9. FT-IR spectra of MEL and its products.

Table 3
Contact angles, surface free energies and polarities of the materials.

Samples	Θ_{water} [°]	$\Theta_{diiodomethane}$ [°]	γ^d [mN m^{-1}]	γ^p [mN m^{-1}]	γ [mN m^{-1}]	Polarity [%]
MEL	75.3 ± 5.2	16.2 ± 3.3	44.7	9.3	54.0	17.1
MEL spd	72.0 ± 0.0	24.8 ± 2.9	42.2	11.1	53.3	20.9
M	21.3 ± 4.7	17.6 ± 6.4	43.7	34.0	77.7	43.7
M spd	20.1 ± 5.0	24.9 ± 5.1	41.6	35.1	76.7	45.7
MEL–M	54.9 ± 6.1	23.9 ± 2.8	42.2	19.3	61.5	31.4
MEL–M–T	19.1 ± 1.4	16.4 ± 0.2	44.0	34.6	78.5	44.0
MEL–M–PVP	26.4 ± 4.6	28.0 ± 1.5	40.6	33.2	73.8	45.0
MEL–M–T + PVP	20.9 ± 3.3	18.4 ± 0.9	43.5	34.7	77.7	44.0

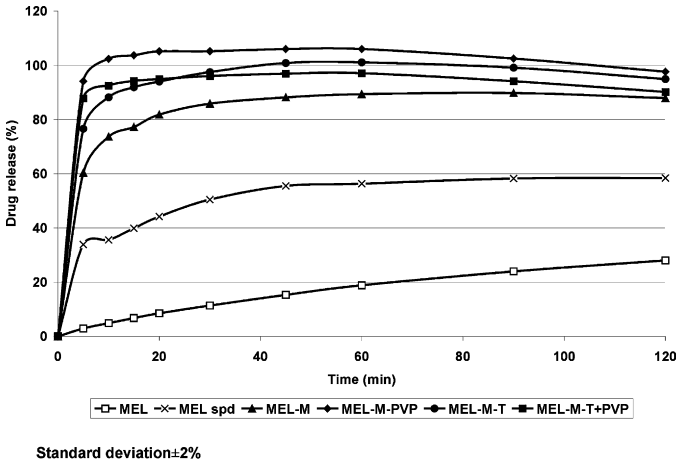

Fig. 10. Dissolution rate of MEL at pH 7.4.

contact angles (19.1° and 20.9°) in both cases and the wetting character could also be perceived. PVP can help stabilize the decreased size and improve the wettability too (26°) [52]. The large surface is hydrophilized by adsorbed stabilizers, as shown by the decreased contact angle. The reduced size and the applied carrier systems are influenced by the surface free energy and the polarity of the initial material. The results of contact angle measurements on samples containing diiodomethane as non-polar component, which provide information about the surface free energies and polarities of the MEL, M and co-spray-dried products, are presented in Table 3. The polarity of MEL spd was increased slightly (20.9%) as compared with the raw MEL. Co-spray-drying with M improved the polarity a little (31.4%). With T and PVP, similar surface free energy and polarity values were manifested as in the case of pure M (~44%).

UV analysis of the *drug content* in the co-spray-dried products confirmed that MEL could be found at a level of 96.5–102% of the theoretically added amount.

The *dissolution* of raw MEL at pH 7.4 (the pH of the intestinal/alveolar/nasal system) was prolonged. MEL spd exhibited the nearly the same profile as that of raw MEL, but the reduced size with the increased specific surface yielded 30% in the dissolution. Fig. 10 presents the dissolution profiles of MEL, MEL spd and the co-spray-dried systems. The products containing the additives gave close to 100% release in the first 5 min. The dissolution in the first 5 min was ~30 times higher than that for MEL. Table 4 presents the drug release from the physical mixtures at 15, 60 and 120 min. The difference could be interpreted in dissolution rate and dissolved concentration of MEL compared the co-spray-dried samples with the physical mixtures. It may be seen that small amounts of additives can play a great role in the dissolution of the drug, and it is therefore important to achieve a correct formulation, but without particle size decreasing these excipients did not give 100% drug release. PVP itself is not such a good wetting agent as Tween. The aggregation inhibition of these excipients is necessary as concerns the particle size decrease and protection, which results in enhanced dissolution. The increased dissolution can be attributed to an increase in surface area as a result of the particle size reduction and to the homogeneous MEL distribution in the carrier-based system. This dissolution tests indicated that the co-spray-dried samples, and especially MEL–M–PVP, resulted in rapid release, furnishing close to 100% of the MEL within 5 min.

Table 4
In vitro drug release of MEL from the physical mixtures.

Samples	15 min [%]	60 min [%]	120 min [%]
MEL	6.80	18.88	28.04
PM–MEL–M	8.13	33.16	55.07
PM–MEL–M–T	46.15	67.85	69.33
PM–MEL–M–PVP	27.88	41.38	43.51
PM–MEL–M–T + PVP	52.57	76.37	78.64

4. Conclusions

The applied carrier-based preparation technique has certain advantages. The method is a non-conventional procedure, which is an organic solvent-free and fast. The particle size and morphology of the API and composites can be optimized via the additives and the process parameters. Instead of the classical approach based on micronization to prepare drug particles (e.g., grinding, crystallization, etc.) followed by blending with a carrier, co-spray-drying of the MEL/M/additives was performed in a one-step process. The dissolved excipients are covered by adsorption and recrystallization the MEL particles to produce solid systems with altered particle size, particle size distribution, morphology and rate of dissolution of the drug. Our results point to an alternative methodology with which to achieve the rapid release of poorly soluble drugs. It appears to be of great potential in pulmonary, nasal, and oral drug delivery systems.

Acknowledgements

"TÁMOP-4.2.1/B-09/1/KONV-2010-0005 creating the Center of Excellence at the University of Szeged" is supported by the European Union and co-financed by the European Regional Development Fund.

References

[1] R. Ambrus, Z. Aigner, C. Soica, C. Peev, P. Szabó-Révész, Amorphisation of niflu-minic acid with polyvinylpyrrolidone prepared solid dispersion to reach rapid drug release, Rev. Chim. 58 (2007) 206–209.
[2] S. Stegemann, F. Leveiller, D. Franchi, H. de Jong, H. Linden, When poor solubility becomes an issue: from early stage to proof of concept, Eur. J. Pharm. Sci. 31 (2007) 249–261.
[3] K.D. Rainsford, Profile and mechanisms of gastrointestinal and other side effects of nonsteroidal anti-inflammatory drugs (NSAIDs), Am. J. Med. (1999) 107–135.
[4] C.A. Lipinski, Drug-like properties and the causes of poor solubility and poor permeability, J. Pharmacol. Toxicol. Methods 44 (2000) 235–249.
[5] H.B. Hassan, M. Kata, I. Erős, Z. Aigner, Preparation and investigation of inclusion complexes containing gemfibrozil and DIMEB, J. Inclusion Phenom. 50 (2004) 219–226.

[6] B.S. Dinesh, B.S. Gleb, Engineered microcrystals for direct surface modification with layer-by-layer technique for optimized dissolution, Eur. J. Pharm. Biopharm. 58 (2004) 521–527.
[7] H.G. Brittain, Effect of mechanical processing on phase composition, J. Pharm. Sci. 91 (2002) 1573–1580.
[8] S. Basavoju, D. Bostro, P.V. Sitaram, Indomethacin–saccharin cocrystal: design, synthesis and preliminary pharmaceutical characterization, Pharm. Res. 25 (2008) 530–541.
[9] A. Gainotti, R. Bettini, A. Gazzaniga, P. Colombo, F. Giordano, Drug-beta-cyclodextrin containing pellets prepared with a high-shear mixer, Drug Dev. Ind. Pharm. 30 (2004) 1061–1068.
[10] M.E. Brewster, T. Loftsson, Cyclodextrins as pharmaceutical solubilizers, Adv. Drug Deliv. Rev. 59 (2007) 645–666.
[11] N. Blagden, M. de Matas, P.T. Gavan, P. York, Crystal engineering of active pharmaceutical ingredients to improve solubility and dissolution rates, Adv. Drug. Deliv. Rev. 59 (2007) 617–630.
[12] S. Shou-Cang, N.G. Kiong, W.L. Chia, Y.C. Dong, B.H. Reginald, Stabilized amorphous state of ibuprofen by co-spray drying with mesoporous SBA-15 to enhance dissolution properties, J. Pharm. Sci. 4 (2010) 1997–2007.
[13] P. Kocbek, S. Baumgartner, J. Kristl, Preparation and evaluation of nanosuspensions for enhancing the dissolution of poorly soluble drugs, Int. J. Pharm. 312 (2006) 179–186.
[14] G. Palmieri, P. Wenrle, A. Stamm, Evaluation of spray-drying as a method to prepare micro particles for controlled drug release, Drug Dev. Ind. Pharm. 20 (1994) 2859–2879.
[15] J. Swarbrick, J. Boylan, Spray drying and spray congealing of pharmaceuticals, in: Encyclopedia of Pharmaceutical Technology, Marcel Dekker, 1992, pp. 207–221.
[16] M. Aulton, Drying, In: Pharmaceutics – The Science of Dosage Form Design, Churchill Livingstone, 2002, 390–395.
[17] T. Hirofumi, Spray-dried composite particles of lactose and sodium alginate for direct tabletting and controlled releasing, Int. J. Pharm. 174 (1998) 91–100.
[18] P. Luger, K. Daneck, W. Engel, G. Trummlitz, K. Wagner, Structure and physicochemical properties of meloxicam, a new NSAID, Eur. J. Pharm. Sci. 4 (1996) 175–187.
[19] Y. Tsubouchi, H. Sano, R. Yamada, A. Hashiramoto, H. Kohno, Y. Kusaka, H. Kondo, Preferential inhibition of cyclooxygenase-2 by meloxicam in human rheumatoid synoviocytes, Eur. J. Pharmacol. 395 (2000) 255–263.
[20] D.E. Frust, Meloxicam: selective COX-2 inhibition in clinical practice, Semin. Arthritis Rheum. 26 (1997) 21–27.
[21] A.P. Goldman, C.S. Williams, H. Sheng, L.W. Lamps, V.P. Williams, M. Pairet, J.D. Morrow, R.N. DuBois, Meloxicam inhibits the growth of colorectal cancer cells, Carciogenesis 19 (1998) 2195–2199.
[22] S. Bavbek, A.B. Dursun, E. Dursun, A. Erylmiaz, Z. Misirligil, Safety of meloxicam in aspirin-hypersensitive patients with asthma and/or nasal polyps, Int. Arch. Allergy Immunol. 142 (2007) 64–69.
[23] A. Bashiri-Shahroodi, P.R. Nassab, P. Szabó-Révész, R. Rajkó, Preparation of solid dispersion by dropping method to improve dissolution rate of meloxicam as poorly water-soluble drug, Drug Dev. Ind. Pharm. 34 (2008) 781–788.
[24] R. Ambrus, P. Kocbek, J. Kristl, R. Sibanc, R. Rajkó, P. Szabó-Révész, Investigation of preparation parameters to improve the dissolution of poorly water-soluble meloxicam, Int. J. Pharm. 381 (2009) 153–159.
[25] P.R. Nassab, R. Rajkó, P. Szabó-Révész, Physicochemical characterization of meloxicam–mannitol binary systems, J. Pharm. Biomed. Anal. 41 (2006) 1191–1197.
[26] N.B. Naidu, K.P.R. Chowdary, K.V.R. Murthy, V. Satyanarayana, A.R. Hayman, G. Becket, Physicochemical characterization and dissolution properties of meloxicam–cyclodextrin binary systems, J. Pharm. Biomed. Anal. 35 (2004) 75–86.
[27] M.H.G. Dehghan, Improving dissolution of meloxicam using solid dispersions, Iranian J. Pharm. Res. 4 (2006) 231–238.
[28] W. Wong, J. Crapper, H.K. Chan, D. Traini, P.M. Young, Pharmacopeial methodologies for determining aerodynamic mass distribution of ultra-high dose inhalers medicines, J. Pharm. Biomed. Anal. 51 (2010) 853–857.
[29] P.R. Nassab, Z.S. Tüske, P. Kása, A. Bashiri-Shahroodi, P. Szabó-Révész, Influence of work of adhesion on dissolution rate in binary solid systems, J. Adhes. 83 (2007) 799–810.
[30] S.N. Campbell Roberts, A.C. Williams, M. Griemsey, S.W. Booth, Quantitative analysis of mannitol polymorphs. X-ray powder diffractometry-exploring preferred orientation effects, J. Pharm. Biomed. Anal. 28 (2002) 1149–1159.
[31] J.D. Castile, W. Lin, A. Smith, P.J. Watts, Intranasal formulations of Meloxicam, GB patent WO/2005/021041 (2005).
[32] Y. Tsubouchi, S. Mukai, Y. Kawahito, R. Yamada, M. Kohno, K.I. Inoue, H. Sano, Meloxicam inhibits the growth of non small cell lung cancer, Anticancer Res. 20 (2000) 2867–2872.
[33] R.F. Souza, K. Shewmake, D.G. Beer, B. Cryer, S.J. Spechler, Selective inhibition of cyclooxygenase-2 suppresses growth and induces apoptosis in human oesophageal adenocarcinoma cells, Cancer Res. 60 (2005) 5767–5772.
[34] H.M.M. Arafa, M.H. Abdel-Wahab, M.F. El-Shafeey, O.A. Badary, F.M.A. Hamada, Anti-fibrotic effect of meloxicam in a murine lung fibrosis model, Eur. J. Pharmacol. 564 (2007) 181–189.
[35] D. Bednarek, A. Szuster-Ciesielska, B. Zdzisinska, M. Kondracki, B. Paduch, M. Kandefer-Szerszen, The effect of steroidal and non-steroidal anti-inflammatory drugs on the cellular immunity of calves with experimentally-induced local lung inflammation, Vet. Immunol. Immunopathol. 71 (1999) 17–28.
[36] H. Kublik, M.T. Vidgren, Nasal delivery systems and their effect on deposition and absorption, Adv. Drug Deliv. Rev. 29 (1998) 157–177.
[37] H.K. Chan, Dry powder aerosol drug delivery – opportunities for colloid and surface scientists, Colloids Surf. A: Physicochem. Eng. Aspects 284–285 (2006) 50–55.
[38] M.J. Telko, A.J. Hickey, Dry powder inhaler formulation, Respir. Care 50 (2005) 1209–1227.
[39] Guidance for Industry Nasal Spray and Inhalation Solution, Suspension, and Spray Drug Products Chemistry Manufacturing, and Controls Documentation, U.S. Department of Health and Human Services Food and Drug Administration Center for Drug Evaluation and Research (CDER), 2002.
[40] P.M. Young, D. Cocconi, P. Colombo, R. Bettini, S. Edge, P. Price, D.F. Steel, M.J. Tobin, Characterisation of surface modified dry powder inhalation carrier prepared by particle smoothing, J. Pharm. Pharmacol. 54 (2002) 1339–1344.
[41] I. Tsujino, T. Yamazaki, M. Masutani, U. Sawada, T. Horie, Effect of Tween 80 on cell killing by etoposide in human lung adenocarcinoma cells, Cancer Chemother. Pharmacol. 43 (1999) 29–34.
[42] B.V. Robinson, F.M. Sullivan, J.F. Borzelleca, S.L. Schwartz, A Critical Review of the Kinetics and Toxicology of Polyvinylpirrolidone (POVIDONE), Lewis Publishers, 1990.
[43] R. Ambrus, A. Pomázi, K. Réti-Nagy, F. Fenyvesi, M. Vecsernyés, P. Szabó-Révész, Cytotoxicity testing of carrier-based microcomposites for DPI application, Pharmazie 66 (2011), doi:10.1691/ph.2011.0378.
[44] I. Gonda, The ascent of pulmonary drug delivery, J. Pharm. Sci. 89 (2000) 940–945.
[45] N. Islam, E. Gladki, Dry powder inhalers (DPIs)-review of device reliability and innovation, Int. J. Pharm. 360 (2008) 1–11.
[46] G. Buckton, Characterisation of small changes in the physical properties of powders of significance for dry powder inhaler formulations, Adv. Drug Deliv. Rev. 26 (1997) 17–27.
[47] G. Palmieri, G. Bonacucina, P. Martino, S. Martelli, Spray-drying as a method for microparticulate controlled release systems preparation: advantages and limits. I. Water-soluble drugs, Drug Dev. Ind. Pharm. 27 (2001) 195–204.
[48] S. Wu, Calculation of interfacial tension in polymer systems, J. Polym. Sci. 34 (1971) 19–30.
[49] E. Oh, P.E. Luner, Surface free energy of ethylcellulose films and the influence of plasticizers, Int. J. Pharm. 188 (1999) 203–219.
[50] T.M. Crowder, J.A. Rosati, J.D. Schroeter, A.J. Hickey, T.B. Martonen, Fundamental effects of particle morphology on lung delivery: predictions of Stokes' law and the particular relevance to dry powder inhaler formulation and development, Pharm. Res. 19 (2002) 239–245.
[51] A. Burger, J.O. Henck, S. Hetz, J.M. Rollinger, A.A. Weissnicht, Energy/temperature diagram and compression behavior of the polymorphs of D-mannitol, J. Pharm. Sci. 89 (2000) 457–468.
[52] R. Zelkó, Á. Orbán, K. Süvegh, Tracking of the physical ageing of amorphous pharmaceutical polymeric excipients by positron annihilation spectroscopy, J. Pharm. Biomed. Anal. 40 (2006) 249–254.